



1 Long Range Plasma Momentum Coupling by High Voltage Static Electric field 2 and Deep Space Exploration

3 Kokwei Chew¹, Xinyu Zhou¹, and Yian Lei¹

4 ¹School of Physics, Peking University, Beijing 100871, China

5 *Correspondence to:* Yian Lei (yalei@pku.edu.cn)

6 **Abstract.** Space exploration has been long constrained by the efficiency and capability of modern chemical rocket. Propellant-
7 less propulsion has been proposed as a solution to expand the boundary of space exploration. In this paper, we examine the
8 possibilities of a propellantless propulsion scheme through the interaction between the spacecraft and ambient plasma. The
9 spacecraft is charged to high electric potential by constantly shooting electrons away. The high voltage spacecraft will deplete
10 the surrounding electrons, thus interact with a wide range of the background plasma (solar wind) and thus effectively extract
11 momentum from the plasma. By taking advantage of the exploitable ambient plasma, a spacecraft can reach very high speed,
12 thus considerably reducing the travel time. The scheme is also applicable for braking, which is helpful in the exploration of
13 inner planets like Venus and Mercury, and the stopping at the destination planets or stars.

14 1 Introduction

15 Space exploration is the next step of human development. The main difficulty experienced in space travel is the long distance
16 across planets, stars, or galaxies, and the low limitation of fuel. The average distance between planets in solar system is about
17 5.5 Astronomical units (AU) or 800 million km away, and the closest star system, the Alpha Centauri is 4.37 light-years ($4.1 \times$
18 10^{16} m) away from solar system. Contemporary spacecraft can hardly reach a speed of 40 kms^{-1} , with the help of multiple
19 slingshot acceleration of the planets. The speed is far too low, considering the travelling to the Alpha Centauri will takes longer
20 than the entire human history.

21 Propellantless propulsion is a scheme proposed to overcome the problems of limited fuels carried by chemical rockets
22 as well as ion thrusters. To date, various kinds of propellantless schemes such as electric sail and solar sail has been proposed
23 as an alternative to chemical rockets for interplanetary or interstellar space travelling. In this paper, we propose a propellantless
24 propulsion scheme by coupling the spacecraft with the ambient plasma to extract its momentum. The spacecraft is charged to
25 high electric potential by constantly shooting electrons far away. The high voltage spacecraft will interact with a wide range
26 of the background plasma (solar wind) in momentum and gain thrust. Comparing with the electric sail proposed by P. Janhunen
27 (2007, 2014), the effective radius of the spacecraft can be held within 100 m to provide better control and manoeuvring.

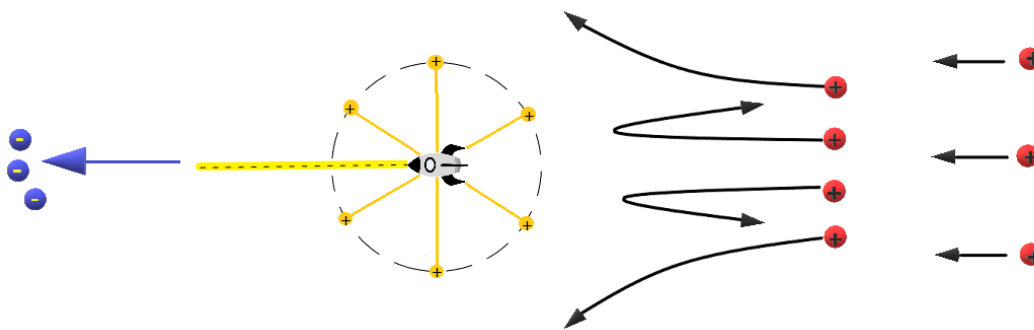
28 The key challenge in the engineering for this scheme is maintaining high potential of the spacecraft. The spacecraft
29 has to accelerate and shot electrons far away to remain high potential and couple with ambient plasma. As electron is the
30 lightest charged particle, with a mass three orders of magnitudes smaller than the lightest ion, hence can be easily deflected by



31 magnets, electron acceleration is the easiest and most durable in engineering. Conventional non-superconducting electron
32 injectors (Bluem et al. 2004) can accelerate electrons to 5 MeV with a compact size, and operate continuously at a maximum
33 current of 1 A. These two parameters set an upper limit on the potential and current of our scheme.
34 The feasibility of maintaining high potential also limited by the field ion evaporation effect or field evaporation (FEV) (Zurlev
35 et al. 2003). FEV is the removal of surface atom from its own lattice structure by induced electric field. The whole process is
36 rather complicated and not well studied yet. In general, when the electric field of a surface exceeded certain threshold, called
37 E^e , there will be significant increase in the FEV process and deplete the structure. A theoretical estimation given by Dinko N.
38 Zurlev (Forbes, 2006) showed that the E^e for most metals is at the order of 10 Vnm^{-1} . For our spacecraft design with an
39 effective radius of 100m, the threshold potential is at the order of 10^{12} V , which is 6 orders of magnitude beyond our limit and
40 thus should not be a problem.

41 2 Concept

42 The spacecraft interact with the ambient plasma through static electric field. Comparing with the electric sail design as
43 proposed by P. Janhunen, our concept consists of a spacecraft located at the centre and linked to several positively charged
44 lightweight balls by conducting tethers. The distance from spacecraft to the balls could be a few hundreds of meters. The
45 spherical shape of balls is designed to reduce the FEV effect, and the distance of the balls is to effectively lower the potential
46 of the structure, hence lower the energy of the ejected electron beam and improve energy efficiency. Due to electric static
47 repulsion; all the balls will distributed uniform around the spacecraft. When deployed for operation, the electron gun is pointed
48 to the opposite or perpendicular direction of the solar wind for ejecting the electrons away from the spacecraft.



49
50 **Figure 1: plasma wind coming from the right side being deflection by the electrostatic field of the spacecraft. The whole structure is**
51 **consisted of a main unit at the center and connected to charged balls attached to the main unit.**

52 For the sake of simplicity in simulation, the whole structure is treated as a sphere with the distance from spacecraft
53 to the balls as the radius of the imaginary sphere. The sphere is charged to a surface potential of V_0 . A stream of plasma (solar
54 wind) moving from the positive x direction. We consider only 1 species of ion, the protons. The deflection of protons from its
55 trajectories provides the momentum. The loss in x-direction momentum of protons is transferred to the spacecraft. To calculate



56 the trajectory and hence the momentum, the potential generated by the sphere need to be addressed. For theoretical estimation,
57 we consider the potential to be a central force and takes the forms of either Coulomb potential or Debye potential.

58 In the absence of plasma, the potential generated by the sphere would be a simple Coulomb potential:

$$59 V(r) = \frac{V_0 r_0}{r}, \quad (1)$$

60 Where r_0 is the radius of the sphere and V_0 is the potential at the surface of the sphere and the potential at far point is zero.
61 Due to the presence of ambient plasma, shielding occurred and the potential dropped by an exponential factor. The effective
62 potential is:

$$63 V(r) = \frac{V_0 r_0}{r} e^{-\frac{r-r_0}{\lambda_D}}, \quad (2)$$

64 Where λ_D is the effective Debye length, $\lambda_D = \sqrt{\epsilon_0(V_0 - V_1)/n_0 e}$ (Janhunen et al. 2016). V_1 is the kinetic energy of the
65 incoming proton.

66 We can estimate thrust by solving the equation of motion of the proton in a Coulomb potential. The deflection or
67 scattering of protons, θ from its original direction is calculated from:

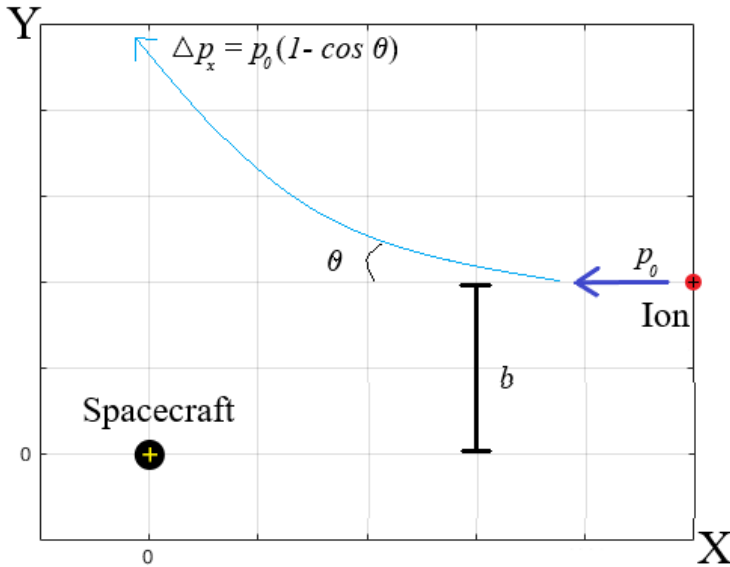
$$68 b = \frac{V_0 r_0 e}{2E_k} \cot \frac{\theta}{2}, \quad (3)$$

69 Where b is the impact parameter, E_k is the kinetic energy of protons in solar wind. In this case, we set θ to 90 degree, the
70 impact parameter b represent how far the electric field can affect and repel the protons from solar wind. Assuming $V_0 = 1$ MV,
71 $r_0 = 100$ m, $E_k = 1.5$ keV, we can have the impact parameter $b = 33$ km and thus an effective scattering cross section of
72 3400 km². The solar wind pressure at 1 AU from the Sun is 2 nPa and the spacecraft is estimated to acquire 6.8 N of thrust at
73 the Earth's orbit.

74 In reality, the potential can never be a symmetric Coulomb potential due to the presence of plasma. The next part of
75 this paper will provide simulation result for the actual thrust obtained by the spacecraft.

76 3 1D Simulation

77 In 1D simulation, the system will reach a static condition after the spacecraft is charged. The particles (ions) interact with the
78 charged spacecraft and eventually the potential around the spacecraft takes the form as described by equation 2. The deflection
79 of protons from its own trajectory contribute the x-direction momentum to the spacecraft. As shown in figure 2, the spacecraft
80 is located at the origin. The ions is coming from the +x direction and assumed to have initial velocity in the x-direction. The
81 motion of the particle calculated by Runge-Kutta method with adaptive time-steps for error control.

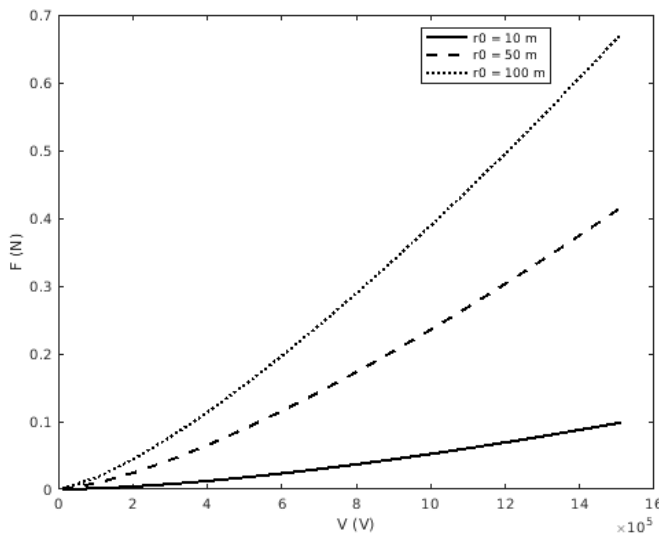


82

83 **Figure 2: The spacecraft located at the origin and the ions from solar wind coming from the positive x direction.**

84

85 The model for 1D simulation is rather simple. It provides the relation between the thrust generated and key parameters
 86 like spacecraft surface potential V_0 , radius r_0 and solar wind density n_0 . This provide a basis for calculating the trajectories for
 87 interplanetary travel for our spacecraft. Figure 3 and table 1 shows the scaling relation between the thrust and surface potential
 of surface as well as solar wind density.



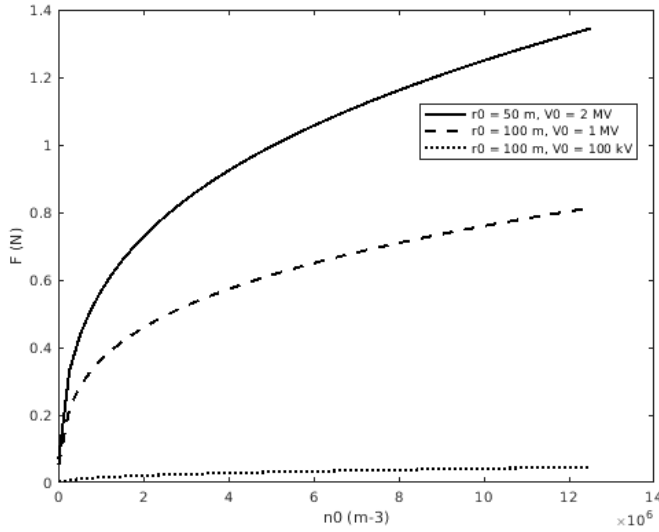
88

89 **Figure 3(a): The relation between thrust F and the surface potential of the sphere V_0 . Dotted line: $r_0 = 100$ m, dashed line: $r_0 =$
 90 50 m, solid line: $r_0 = 10$ m. Plasma density $n_0 = 1.2 \times 10^6 \text{ m}^{-3}$.**

91



92



93

94

95

Figure 3(b): Figure 3(b) The relation between thrust F and the plasma density of solar wind n_0 . Dotted: $r_0 = 50$ m, $V_0 = 2$ MV, dashed: $r_0 = 100$ m, $V_0 = 1$ MV, solid: $r_0 = 100$ m, $V_0 = 100$ kV.

96

Table1: scaling relation between thrust F and V_0 , n_0 , r_0 .

$n_0 / 10^5 \text{ m}^{-3}$	V_0 / V	r_0 / m	Scaling
5.0	-	10	$F \propto V_0^{1.4715}$
5.0	-	50	$F \propto V_0^{1.3257}$
5.0	-	100	$F \propto V_0^{1.2771}$
1.0	-	100	$F \propto V_0^{1.3290}$
-	100 k	10	$F \propto n_0^{0.5723}$
-	100 k	100	$F \propto n_0^{0.4360}$
-	1.0 M	10	$F \propto n_0^{0.5330}$
-	1.0 M	50	$F \propto n_0^{0.3724}$
-	1.0 M	100	$F \propto n_0^{0.3183}$
5.0	100 k	-	$F \propto r_0^{0.8603}$
1.0	1.0 M	-	$F \propto r_0^{0.6804}$
5.0	1.0 M	-	$F \propto r_0^{0.6804}$

97

98

99

100

To estimate the electrons flux, we use the Orbital Motion Limited (OML) theory ^{[1][10]}. An electron will be captured when its trajectory meets the surface of the sphere. The electrons from solar wind coming from 1 direction, if the impact parameter (distance of electron from centre of sphere and perpendicular to its own velocity) lies within certain value, the



101 electron will be absorbed by the sphere. Assuming that the electrons only come from solar wind, and experience a central force.

102 With simple mechanic invariants, we can calculate the current:

103
$$I = \pi r_s^2 e n_0 v, \quad (4)$$

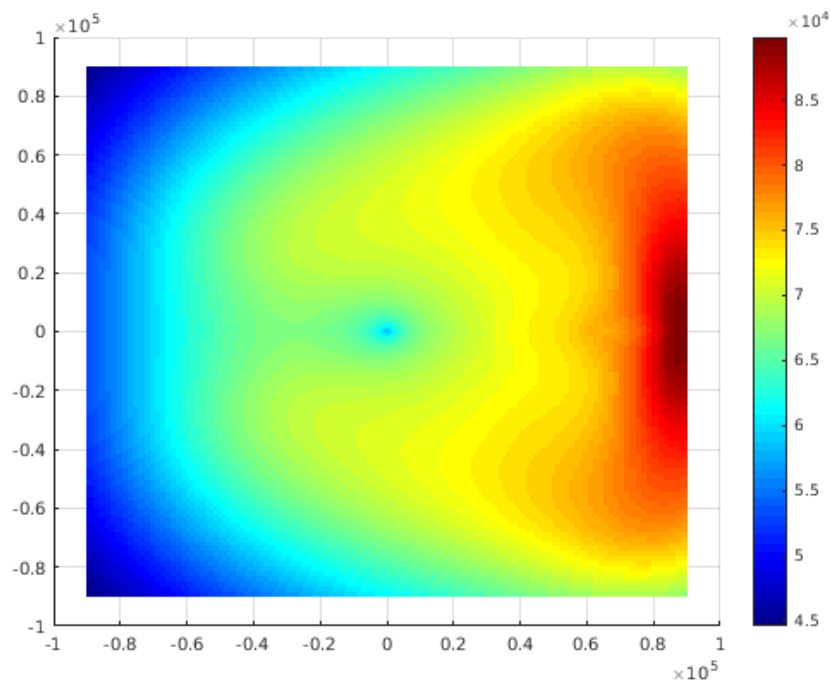
104 Where n_0 is the density of the electron in solar wind, v is the velocity of incoming electron. $r_s = r_0 \sqrt{1 + \frac{2eV_0}{mv^2}}$ is the impact
105 parameter. All electrons aimed at impact parameter less than r_s will hit on the surface of the sphere.

106 4 2D Simulation

107 In this section, we provide a PIC 2D simulation describe the behavior of the particles. The simulation region is has a cylindrical
108 symmetry along the x -axis. Similar to figure 2, both the protons and electrons constantly flow in from the $+x$ direction. The
109 electric field is solved by Coulomb equation. The potential of the sphere (spacecraft) is V_0 . All the electrons moving inside the
110 sphere are absorbed.

111 The simulation span across a region of 18 km * 9 km, with spatial grid varying linearly from 10 m to 1800 m. The
112 grid size is small at the origin to provide a more precise result around the spacecraft. With plasma density of $n_0 = 5.0 \times$
113 10^4 m^{-3} , the Langmuir frequency for electron is equivalent to $\omega_{pe} = 1.3 \times 10^4 \text{ s}^{-1}$. The timestep is set to $\Delta t = 7.75 \times$
114 10^{-5} s . We run 2 cases, (1) $V_0 = 1 \text{ MV}$, $r_0 = 100 \text{ m}$, (2) $V_0 = 2 \text{ MV}$, $r_0 = 50 \text{ m}$, with $T = 32000 \Delta t$.

115 Figure 4 shows the established stable contour plot of the potential. We can see there is a high potential area on the
116 incoming side of the solar wind. This means the spacecraft can couple or interact with a large range of the ambient plasma.
117 Figure 4(b) is for ion density. The concentration of ions on the right side is because the ions have nowhere to go. Figure 4(c)
118 is for electron density; note the high concentration of electrons around the spacecraft.

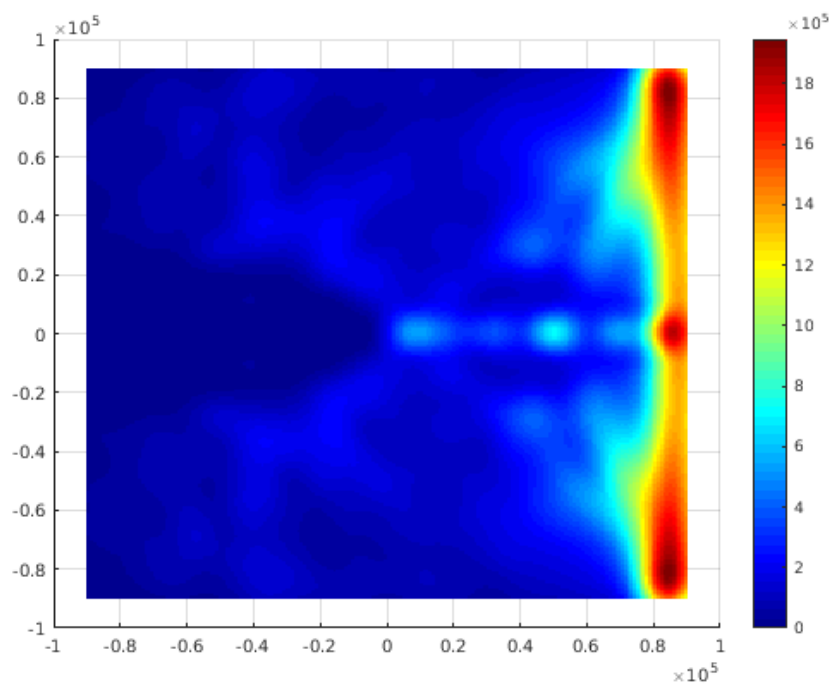


119

120

121

Figure 4(a): The plasma potential when simulation reached static state ($T = 32000 \Delta t$, $\Delta t = 7.75 \times 10^{-5}$ s), the spacecraft located at the origin.

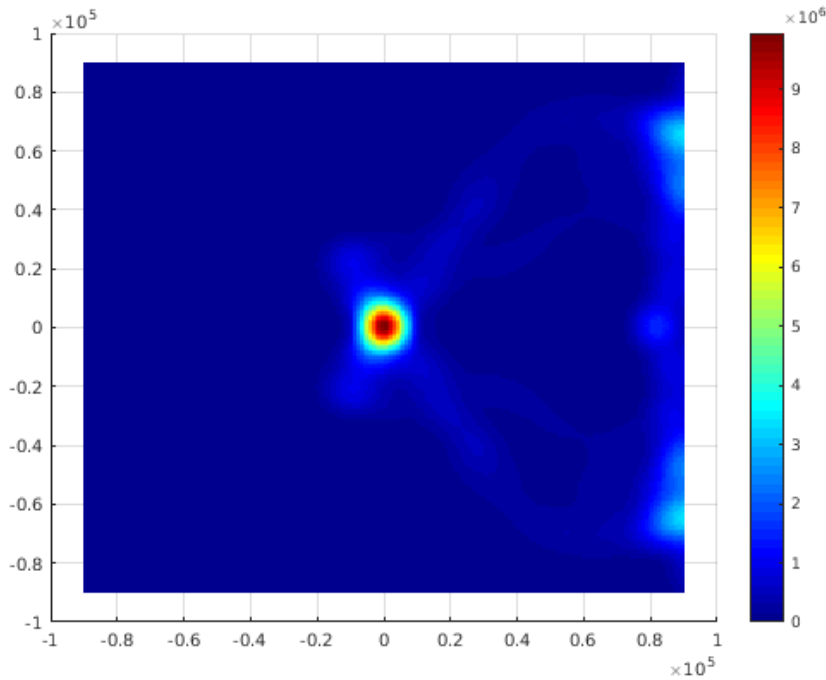


122



123
 124

Figure 4(b): The ion density when simulation reached static state. Ions is repelled by the sphere, hence low ion density at the left side. A large portion of ions accumulation at the right side of the region is due to the boundary effect.



125
 126

Figure 4(b): The electron density when simulation reached static state. Electrons in the region almost depleted.

127
 128
 129
 130
 131

The thrust acting on the sphere and the electron current is calculated and compared with 1D simulation in table 2. In 2D simulation, the thrust is 2~3 times larger than that of 1D simulation, and the electron current lower. Hence, the momentum coupling between the spacecraft and the ambient plasma is stronger than plasma shielding.

Table 2: Comparison between 1D and 2D simulation result.

V_0, r_0	1D Simulation		2D Simulation	
	Thrust / N	Current / mA	Thrust / N	Current / mA
1 MV, 100 m	0.52	168	1.6	102
2 MV, 50 m	0.77	84	1.6	73

132

5 Interplanetary Travel

133
 134

In this section, we consider a simplified journey starting from Earth's orbit to outer planet such as Mars and Jupiter. A comparison between result from 1D and 2D simulation showed that the 1D still a good approximation for thrust calculation.



135 The thrust generated depends on the ambient plasma density n_0 , and n_0 drops by inversely square law of the distance, D , from
 136 the Sun.

137 Assuming

$$138 \quad F(D) = A \cdot D^k, \quad (5)$$

139 Where F is the thrust, D is the distance to the Sun. k is a scaling coefficient obtained from 1D simulation. A is a
 140 constant determined by 2D simulation. From 1D simulation, k is within the range from -1.3 to -1.5. Adding the force into the
 141 equation of motion of the spacecraft:

$$142 \quad m(\ddot{D} - D\dot{\theta}^2) = -\frac{GM_S m}{D^2} + F(D), \quad (6)$$

143 Where M_S and m are the mass of the Sun and spacecraft respectively, θ is the angular coordinate of the spacecraft in
 144 a polar coordinate system with the Sun located at the center. By solving the equation of motion numerically with initial distance
 145 being the radius of the orbit of the Earth, radial velocity being zero and tangential velocity equal to that of Earth, we can
 146 calculate the trajectories of the spacecraft. Table 3 shows the time taken for each mission under various circumstances. The
 147 main power consumption is from the electron accelerator (gun).
 148

Table 3: Time taken for spacecraft to a journey to reach different planets.

V_0 (MV)	r_0 (m)	m (kg)	Initial acceleration (mms^{-2})	Time taken (days)				Power (kW)
				Mars	Jupiter	Saturn	Pluto	
0.1	100	59	0.85	267	-	-	-	11
1	100	500	3.64	80	290	446	1055	102
1	100	1000	1.82	120	503	774	1758	102
2	50	500	4.02	76	277	430	1039	73
2	50	1000	2.01	114	471	732	1717	73

149
 150 The most efficient way for sending spacecraft to a target planet is by orbit transfer [11]. The spacecraft is transfer
 151 from a smaller orbit (Earth) to a larger orbit (Mars) following a Hohmann transfer orbit. In our case, for planets like the Mars,
 152 the spacecraft can follow a similar orbit for energy efficiency. With a surface potential $V_0 = 1$ MV, effective radius $r_0 = 100$ m,
 153 a spacecraft of mass $m = 460$ kg can be transferred to the Mars.

154 6 Result and discussions



155 We proposed an ambient plasma momentum coupling spacecraft propelling scheme by utilizing high electric potential for the
156 spacecraft to interact with a wide range of background plasma, which can be considered as a compact electric sail with a much
157 smaller structure.

158 Preliminary calculations show that it is promising in space exploration. There are some discrepancies between the 1D
159 and 2D simulation but generally, the order of the thrust and electron current are the same. The 2D simulation result shows that
160 with a surface potential of the spacecraft of 1 MV, this scheme can produce a thrust of about 1.6 N, by consuming a power of
161 about 100 kW. The thrust-energy efficiency is comparable to contemporary plasma thrusters (Mason et al. 2001, Richard 2004).
162 The simulation is performed in low plasma density. In reality, this scheme could generate a larger thrust than our calculation.
163 Since this scheme requires no propellant, it has an advantage over chemical rockets and ion thrusters. Comparing with the E-
164 sail proposed by P. Janhunen, our spacecraft require a relatively small structure (100 m versus 10 km). It is much easier to
165 control or manoeuvre. A simple calculation shows that a spacecraft of 500 kg can reach Mars in 80 days and Pluto in 3 years.

166 The scheme is also applicable in braking, as long as the momentum of ambient plasma is exploitable. In situations
167 like braking near Jupiter, travelling to the inner planets, the plasma trapped by Jupiter and the solar wind can be used for
168 braking.

169 This scheme can achieve very high interstellar travelling speed by delivering artificial dense and energetic beams to
170 the spacecraft over a very long distance, by, for example, a series of powerful particle accelerators on the Moon, other satellites,
171 or dwarf planets, thus drastically shorten the travelling time to the nearest stars from tens of thousands of years to a few
172 hundreds of years.

173 If the situation is favorable, such as in a cosmic jet, a spacecraft could be accelerated to relativistic velocities.

174 References

- 175 Bleum, H. et al.: Electron Injectors for Next Generation X-Ray Sources, SPIE 49th Arizual Mtg., Denver, CO, 2-6 August
176 (2004).
- 177 Forbes, R.G.: Extraction of Experimental ZERO-Q Evaporation Field Values, 15th Annual User Workshop of University of
178 Surrey Ion Beam Centre, Guildford, UK, 2006, 545.
- 179 Janhunen, P.: Electric sail for spacecraft propulsion, *Journal of Propulsion and Power*, 20(4), 763–764, 2004.
- 180 Janhunen, P.: Coulomb drag devices: electric solar wind sail propulsion and ionospheric deorbiting, *Space Propulsion 2014*,
181 Köln, Germany, May 19-22, 2014b, available at: <http://arxiv.org/abs/1404.7430>, 2014.
- 182 Janhunen, P.: Boltzmann electron PIC simulation of the E-sail effect, *Ann. Geophys.*, 33, 1507-1512, 2015.
- 183 Janhunen, P. and Sandroos A.: Simulation study of solar wind push on a charged wire: basis of solar wind electric sail
184 propulsion, *Ann. Geophys.*, 25, 755–767, 2007.
- 185 Janhunen, P. and Toivanen P.: Safety criteria for flying E-sail through solar eclipse, *Acta Astronautica*, available at:
186 <http://arXiv:1502.04557>, 2015.



- 187 Janhunen, P., et al.: Electric solar wind sail: towards test missions, *Rev. Sci. Instrum.*, 81, 111301, 2010.
- 188 Janhunen, P. et al.: Electric solar wind sail applications overview, available at: <https://arxiv.org/abs/1604.08414>, 2014.
- 189 Janhunen, P. et al.: CUBESAT testing of Coulomb drag propulsion, available at: <https://arxiv.org/abs/1604.08414>, 2016.
- 190 Mason, L. S. et al.: 1000 hours of testing on a 10 kilowatt hall effect thruster, 2001, American Institute of Aeronautics &
191 Astronautics, AIAA 2001-3773, 2001.
- 192 Richard, R. H., Development and characterization of high-efficiency, high-specific impulse xenon hall thrusters, NASA/CR—
193 2004-213099., 2004
- 194 Tang, X.Z., Delzanno G.L.: Orbital-motion-limited theory of dust charging and plasma response, available at:
195 <https://arxiv.org/abs/1503.07820>, 2015
- 196 Zurlev, D. N. et al.: Field ion emission: the effect of electrostatic field energy on the prediction of evaporation field and
197 charge state, *J. Phys. D: Appl. Phys.* **36** (2003) L74–L78, 2003.
- 198